Evaluating the angular power spectrum of cortical folding

Christopher R. Madan (christopher.madan@nottingham.ac.uk)
School of Psychology, University of Nottingham
Nottingham NG7 2RD, United Kingdom

Abstract

The most defining feature of the cortex is its folding structure. While these peaks and valleys can be coarsely characterised using measures of cortical structure such as gyrification and fractal dimensionality, these are not directly sensitive to the different scales of folding that comprise the brain's cortical structure. Here we developed an approach for characterising the angular power spectrum of cortical folding using spherical harmonics and informed by prior research investigating the cosmic microwave background. In this work, we ultimately yielded a single summary measure that is sensitive to minor folds along the cortical gyri and sulci and is sensitive to age-related differences in cortical structure.

Keywords: brain morphology; spherical harmonics; cortex; MRI; topological spatial frequency; gyrification

Introduction

The most defining feature of the cortex is its folding structure. An on-going challenge is to develop useful measures to characterise the folding pattern of the cortex and how individual brains may differ in their folding. Currently, the most established approach is a measure of gyrification (Armstrong, Schleicher, Omran, Curtis, & Zilles, 1995; Zilles, Armstrong, Schleicher, & Kretschmann, 1988), which is based on the ratio of cortical surface area relative to an estimated smooth surface that encloses the cortex. Sulci can also be identified and then quantified based on their width and depth (Madan, 2019a). Another approach is to treat the cortex as a complex natural structure and quantify its complexity using fractal geometry (Hofman, 1991; Kiselev, Hahn, & Auer, 2003). Recent findings have demonstrated that these approaches can be useful in characterising cortical structure and age-related differences in cortical structure (Madan & Kensinger, 2016, 2018).

Here we propose an alternative measure, the angular power spectrum of cortical folding. This approach relies on spherical harmonics, where the cortical structure is reconstructed using basis functions that vary in their topological spatial frequency of folding. This approach complements recent work to develop novel measures of brain morphology for subcortical structures (Madan, 2019b), with the overarching aim of improving our understanding of individual differences in brain structure associated with healthy aging, neurological disorders, cognitive abilities, and other inter-individual differences.

Methods

Calculation

As a Fourier approach can be used to approximate a complex natural linear function using weighted combinations of sinusoidal functions, spherical harmonics can be used to reconstruct complex structures through weighted summation of spherical harmonic bases that vary in topological frequency (degree, ℓ) and polarity (order, m). Figure 1 illustrates the spherical harmonics bases for positive orders.
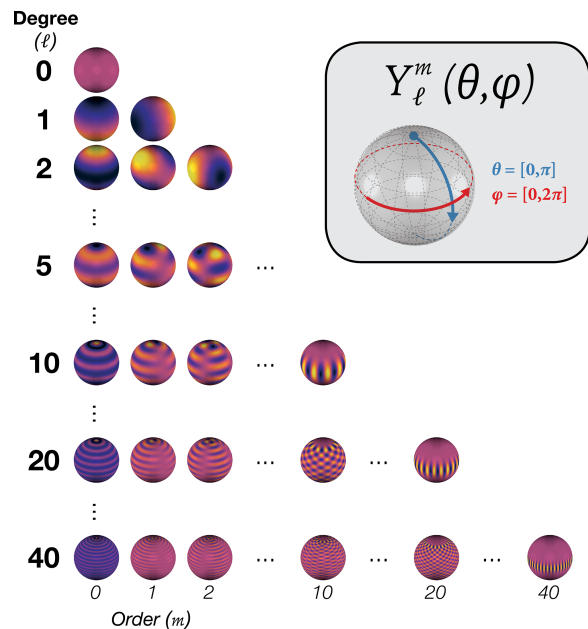

Figure 1: Illustration of the spherical harmonic multipole components (i.e., bases), for positive orders. Components with negative orders appear analogous to the positive-order components, but with different polarity orientations.

Multipole components Spherical harmonics are based on an underlying spherical coordinate system, where θ ranges from one pole to another (i.e., $[0,\pi]$ or $180°$, akin to latitude) and φ wraps around the 'equator' (i.e., $[0,2\pi]$ or $360°$, akin to longitude) following Euler angle conventions, as shown in the inset of Figure 1. Degree ℓ denotes the degree of the spherical harmonic multipole, with larger values corresponding to higher topological spatial frequencies. $\ell = 0$ has no poles, $\ell = 1$ has a singular polarity gradient (akin to a magnet). Higher degrees, corresponding to multiple poles, have more complicated arrangements but in combination can be used to
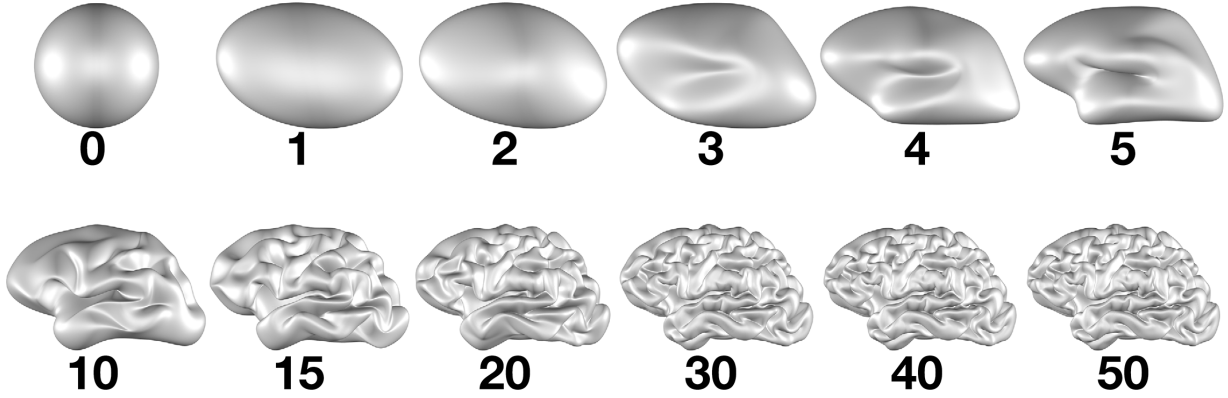
Figure 2: Cortical reconstructions for a representative brain based on spherical harmonics. Each panel was set with a maximum on the spherical harmonic degree (ℓ_{max}) available for approximating the cortical surface.

approximate complex three-dimensional structures, including the folding pattern of a human cortical surface, as in Figure 2.

Each degree ℓ has orders m from $-\ell$ to ℓ, yielding $2\ell+1$ components for each degree. When constructing a complex structure using spherical harmonics, each combination of degree–order, which are individually referred to as multipole components or bases, is multiplied with a corresponding set of weights ($a_{\ell m}$), corresponding to the amplitudes for each ℓ, m component. Due to the spherical system, unlike Fourier bases, spherical harmonic multipole components can present as distinct types of patterns, referred to as zonal (e.g., $\ell=20$, $m=0$ in Figure 1), sectorial (e.g., $\ell=20$, $m=20$), and tesseral (e.g., $\ell=20$, $m=10$). The pattern of each multipole component, $Y_\ell^m(\theta, \varphi)$, is defined as:

$$Y_\ell^m(\theta,\varphi) = \begin{cases} c_{\ell m} P_\ell^{|m|}(\cos\theta)\sin(|m|\varphi), & -l \leq m \leq -1 \\ \frac{c_{\ell m}}{\sqrt{2}} P_\ell^{|m|}(\cos\theta), & m=0 \\ c_{\ell m} P_\ell^{|m|}(\cos\theta)\cos(|m|\varphi), & 1 \leq m \leq l \end{cases} \tag{1}$$

where $P_\ell^{|m|}$ is the Legendre polynomial of degree ℓ and order m, and $c_{\ell m}$ is a normalisation factor, $\sqrt{((2\ell+1)/2\pi)((\ell-|m|)!/(\ell+|m|)!)}$.

Spherical harmonic cortical reconstruction Cortical surfaces can be reconstructed using spherical harmonics, as has been done in previous studies (e.g., Chung, Dalton, Shen, Evans, & Davidson, 2007; Madan & Kensinger, 2017; Williams, El-Baz, Nitzken, Switala, & Casanova, 2012). Here, spherical harmonic multipole component amplitudes, $a_{\ell m}$, were fit to the FreeSurfer cortical meshes using a weighted Fourier series approach, following the method described in Chung et al. (2007) and code from Chung (2014). This approach relies on a heat kernel smoothing method with a defined maximum spherical harmonic degree, $\ell_{max} = 50$, and bandwidth, $\sigma = .001$. Weighted spherical harmonics are a generalised form of traditional spherical harmonics that reduces ringing artifacts related to the Gibbs phenomenon

(Chung, 2014; Chung et al., 2007). Note, here we reconstructed hemispheres individually, rather than whole brains as others have done (e.g., Chung et al., 2007; Williams et al., 2012), as this was considered to be more representative of actual cortical folding patterns (e.g., Madan & Kensinger, 2017). As such, the angular power spectrum will be influenced by being calculated on either the combined bilateral cortical surface or individual hemispheres and then averaged across the two.

To illustrate the incremental contributions of increasing degrees of spherical harmonic components, a representative cortical surface was reconstructed with varying maximum spherical harmonic degree, ℓ_{max}, shown in Figure 2.

Angular power spectrum The relationship between the spherical harmonic degree ℓ and the angular scale of the cortical folding (in degrees, λ) is defined by $180°/\ell$. This corroborates the visual pattern evident in Figure 2: High power at $\ell=1$ (or $\lambda=180°$) corresponds to overall elongation of the sphere in to a ellipsoid, while $\ell=2$ (or $\lambda=90°$) adds an additional folding component in the orthogonal axis. The addition of further degrees of spherical harmonics yields a structure similar to an inflated brain surface at $\ell=4$. Major gyri are observable in the range of degrees $\ell=10$ through 15, corresponding to angular folding of approximately $12-18°$. Minor folds along the gyri are visible starting from approximately $\ell=30$ (or $\lambda=6°$).

The power for each spherical harmonic degree ℓ, C_ℓ, is defined as the mean of the power across the $2\ell+1$ multipole components:

$$C_\ell = \frac{1}{2\ell+1} \sum_{m=-\ell}^{\ell} |a_{\ell m}|^2 \tag{2}$$

This equation is consistent with previous work on spherical harmonics (e.g., Hinshaw et al., 2003). Note that the power spectrum in studies of the cosmic microwave background is often plotted re-scaled as $\ell(\ell+1)C_\ell/2\pi$ (Hinshaw et al., 2003; Nolta et al., 2009; Souradeep, Saha, & Jain, 2006; Tegmark, 1997) or the square root of this value (Miller et al., 1999;

Tegmark, 1997), however, this is intended to normalise for the initial conditions and inflation of the universe (i.e., the Sachs-Wolfe plateau, $\ell \lesssim 100$) which is not relevant to the current investigation. The power spectrum of cortical folding is shown in the upper portion of Figure 3.
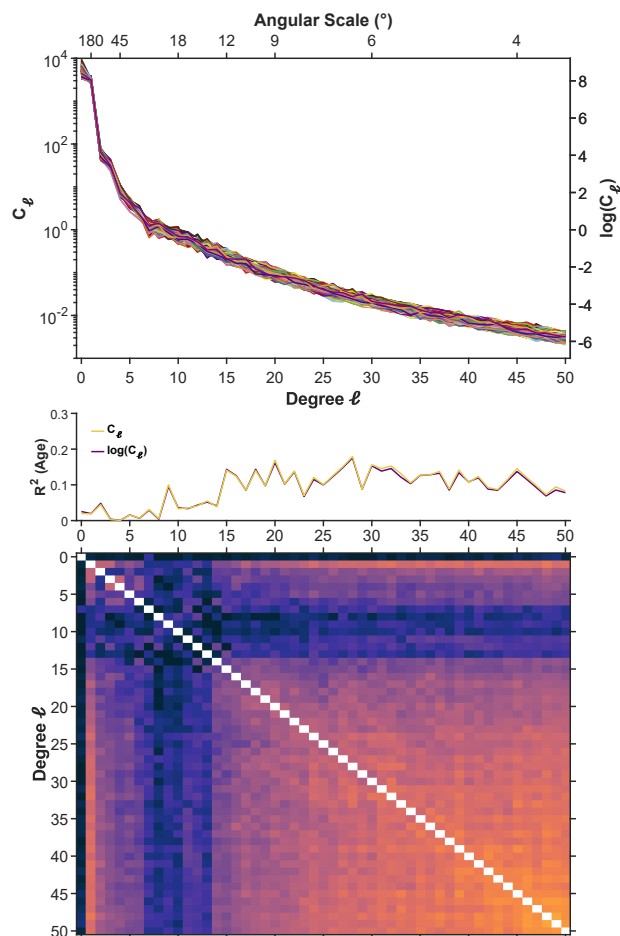

Figure 3: Angular power spectrum of cortical folding.
Top: Angular power spectrum for degrees ℓ from 0 to 50 from the DLBS dataset. Power, C_ℓ, was plotted on a semilog scale to better show the power of high frequency degrees; $\log(C_\ell)$ shown on the right y-axis. Angular scale is plotted along the upper x-axis to aid in interpretation (see main text). Each coloured line represents an individual participant's cortical folding power spectrum.
Middle: R^2 values for the relationship between degree ℓ and age for C_ℓ and $\log(C_\ell)$, note the high degree of consistency.
Bottom: Pairwise correlations, r, between $\log(C_\ell)$ values for all combinations of degree ℓ; brighter values indicate higher correlations.

Summarising the power spectrum To make this power spectrum measure more straightforward to use as a gross measure of cortical structure for inter-individual difference analyses, we sought to determine a single summary measure. R^2 values between the power, C_ℓ, and age were relatively consistent for degrees ℓ of 15 and higher, as shown in Figure 3 (middle). However, as untransformed values, power C_ℓ decreases drastically in relation to degree ℓ. To make variations in angular power more comparable across degrees, power values were log-transformed, see upper portion of Figure 3 (right y-axis). This transformation had a negligible effect on the R^2 values for individual degrees, but would make averaging across degrees more consistent (rather than being more heavily weighted on the larger power on the lower topological spatial frequencies/higher angular scales. Taken together, we developed γ as a summary measure of the angular power spectrum of cortical folding:

$$\gamma\left(\ell_{min}, \ell_{max}\right) = \frac{1}{\ell_{max} - \ell_{min} + 1} \sum_{\ell=\ell_{min}}^{\ell_{max}} \log(C_\ell) \qquad (3)$$

A number of other summary statistics were examined, e.g., fitting a decreasing power function to the power spectrum values, but these were found to be less sensitive to inter-individual differences in cortical structure.

Dataset

Data consisted of 315 healthy adults (198 females), aged 20–89, from wave 1 of the Dallas Lifespan Brain Study (DLBS). Participants were screened for neurological and psychiatric issues. All participants scored 26 or above on the MMSE. T1 volumes were acquired using a Philips Achieva 3 T with a MPRAGE sequence. Scan parameters were: TR=8.1 ms; TE=3.7 ms; flip angle=12°; voxel size=1×1×1 mm. See Kennedy et al. (2015) for further details about the dataset.

Preprocessing of MRI data

The T1-weighted structural MRIs were processed using FreeSurfer v6.0 (Fischl, 2012). Surface meshes were estimated using the standard processing pipeline, i.e., `recon-all`, and no manual edits were made to the surfaces. 1 participant (female) was excluded from further analyses due to a failure to reconstruct the cortical surface.

Results

The overall angular power spectrum of cortical folding is shown in the upper portion of Figure 3. This approach to characterising cortical structure has never been done before.

As the R^2 values for individual degrees ℓ with age are relatively consistent for both C_ℓ and $\log(C_\ell)$ are highly consistent, the log measure appears preferable. The mean correlation of C_ℓ for degrees 15 through 50 is $-.343$; the same measure for $\log(C_\ell)$ is $-.338$. However, if the mean C_ℓ is calculated first and then correlated with age, as opposed to averaging across correlation statistics, is $-.508$; again, the comparable statistic

for $\log(C_\ell)$ is $-.458$. Despite this small decrease in correlation strength, the $\log$ transformation increases the sensitivity of the correlation to amplitudes of the higher degrees. Here we consider this more uniform influence of degree ℓ to be preferable as a summary statistic, even though power at higher degrees was slightly less related to age effects. Table 1 lists a series of correlations conducted to aid in evaluating the relationship between angular power spectrum and age, though further development is needed. As visible in the lower portion of Figure 3, there appear to be several distinct components to the relationship between power at different degrees.

		Correlation (r)	
ℓ_{min}	ℓ_{max}	C_ℓ	$\log(C_\ell)$
15	50	$-.508$	$-.458$
15	30	$-.508$	$-.499$
30	50	$-.442$	$-.410$
0	0	$+.140$	$+.159$
1	5	$-.141$	$-.150$
8	12	$-.286$	$-.321$

Table 1: Correlation values between mean angular power spectrum and age, for degrees between ℓ_{min} and ℓ_{max}, both with and without $\log$ transformation.

Conclusion

While many features of cortical structure are known to differ in relation to inter-individual differences, here we developed a novel measure based on the angular power spectrum of cortical folding, γ. The primary aim is that additional measures of structure will capture unique sources of variance and allow us to better understand how inter-individual factors are reflected in brain structure (see Madan & Kensinger, 2018, and Madan, 2019b, for related investigations). Further work will be necessary to explore how this measure relates to other measures of cortical structure–such as cortical thickness, gyrification, sulcal morphology, and fractal dimensionality.

Acknowledgments

References

Armstrong, E., Schleicher, A., Omran, H., Curtis, M., & Zilles, K. (1995). The ontogeny of human gyrification. *Cerebral Cortex*, *5*, 56–63. doi: 10.1093/cercor/5.1.56

Chung, M. K. (2014). *Statistical and computational methods in brain image analysis*. CRC Press.

Chung, M. K., Dalton, K. M., Shen, L., Evans, A. C., & Davidson, R. J. (2007). Weighted Fourier series representation and its application to quantifying the amount of gray matter. *IEEE Transactions on Medical Imaging*, *26*, 566–581. doi: 10.1109/tmi.2007.892519

Fischl, B. (2012). FreeSurfer. *NeuroImage*, *62*, 774–781. doi: 10.1016/j.neuroimage.2012.01.021

Hinshaw, G., Spergel, D. N., Verde, L., Hill, R. S., Meyer, S. S., Barnes, C., . . . Wright, E. L. (2003). First-year Wilkinson Microwave Anisotropy Probe (WMAP) observations: The angular power spectrum. *Astrophysical Journal Supplement Series*, *148*, 135–159. doi: 10.1086/377225

Hofman, M. A. (1991). The fractal geometry of convoluted brains. *Journal für Hirnforschung*, *32*, 103–111.

Kennedy, K. M., Rodrigue, K. M., Bischof, G. N., Hebrank, A. C., Reuter-Lorenz, P. A., & Park, D. C. (2015). Age trajectories of functional activation under conditions of low and high processing demands: An adult lifespan fMRI study of the aging brain. *NeuroImage*, *104*, 21–34. doi: 10.1016/j.neuroimage.2014.09.056

Kiselev, V. G., Hahn, K. R., & Auer, D. P. (2003). Is the brain cortex a fractal? *NeuroImage*, *20*, 1765–1774. doi: 10.1016/s1053-8119(03)00380-x

Madan, C. R. (2019a). Robust estimation of sulcal morphology. *Brain Informatics*. doi: 10.1186/s40708-019-0098-1

Madan, C. R. (2019b). Shape-related characteristics of age-related differences in subcortical structures. *Aging & Mental Health*, *23*, 800–810. doi: 10.1080/13607863.2017.1421613

Madan, C. R., & Kensinger, E. A. (2016). Cortical complexity as a measure of age-related brain atrophy. *NeuroImage*, *134*, 617–629. doi: 10.1016/j.neuroimage.2016.04.029

Madan, C. R., & Kensinger, E. A. (2017). Test–retest reliability of brain morphology estimates. *Brain Informatics*, *4*, 107–121. doi: 10.1007/s40708-016-0060-4

Madan, C. R., & Kensinger, E. A. (2018). Predicting age from cortical structure across the lifespan. *European Journal of Neuroscience*, *47*, 399-416. doi: 10.1111/ejn.13835

Miller, A. D., Caldwell, R., Devlin, M. J., Dorwart, W. B., Herbig, T., Nolta, M. R., . . . Tran, H. T. (1999). A measurement of the angular power spectrum of the cosmic microwave background from $l = 100$ to 400. *Astrophysical Journal*, *524*, L1–L4. doi: 10.1086/312293

Nolta, M. R., Dunkley, J., Hill, R. S., Hinshaw, G., Komatsu, E., Larson, D., . . . Wright, E. L. (2009). Five-year Wilkinson Microwave Anisotropy Probe observations: Angular power spectra. *Astrophysical Journal Supplement Series*, *180*, 296–305. doi: 10.1088/0067-0049/180/2/296

Souradeep, T., Saha, R., & Jain, P. (2006). Angular power spectrum of CMB anisotropy from WMAP. *New Astronomy Reviews*, *50*, 854–860. doi: 10.1016/j.newar.2006.09.009

Tegmark, M. (1997). How to measure CMB power spectra without losing information. *Physical Review D*, *55*, 5895–5907. doi: 10.1103/physrevd.55.5895

Williams, E., El-Baz, A., Nitzken, M., Switala, A., & Casanova, M. (2012). Spherical harmonic analysis of cortical complexity in autism and dyslexia. *Translational Neuroscience*, *3*, 36–40. doi: 10.2478/s13380-012-0008-y

Zilles, K., Armstrong, E., Schleicher, A., & Kretschmann, H.-J. (1988). The human pattern of gyrification in the cerebral cortex. *Anatomy and Embryology*, *179*, 173–179. doi: 10.1007/bf00304699